MICROSTRUCTURAL EVALUATION OF PORTLAND CEMENT TERNARY PASTE WITH NANOSILICA (NS) AND METAKAOLIN (MK) AT EARLY HYDRATION AGES

Jayme de Melo Ribeiro [1], Divino Gabriel Lima Pinheiro [2], João Henrique da Silva Rêgo[3], Fernando Pelisser [4], Moisés Frias Rojas [5] and Amparo Moragues Terrades [6]

[1] Department of Civil and Environmental Engineering, University of Brasília (UnB), Brasília 70910-900, Brazil
jaymemrufpa@gmail.com
[2] Department of Civil and Environmental Engineering, University of Brasília (UnB), Brasília 70910-900, Brazil
divino.pinheiro@ifg.edu.br
[3]Department of Civil and Environmental Engineering, University of Brasília (UnB), Brasília 70910-900, Brazil
jhenriquerego@unb.br
[4] Department of Civil Engineering, Laboratory of Application of Nanotechnology in Civil Construction (LabNANOTEC), Federal University of Santa Catarina (UFSC), Florianópolis 88040-900, Brazil
pelisser@hotmail.com
[5] Eduardo Torroja Institute for Construction Sciences (IETcc), Spanish National Research Council, 28033 Madrid, Spain
mfrias@ietcc.csic.es
[6] Department of Civil Engineering: Construction, Polytechnic University of Madri, Calle del Prof. Araguren, 3, 28040 Madrid, Spain
amparo.moragues@upm.es

ABSTRACT

The production of high-performance cementitious compounds with supplementary cementitious materials (SCM), such as metakaolin (MK) and nanosilica (NS), can generate synergistic effects on the cementitious matrix, altering the properties and molecular structure of C-S-H, especially at early hydration ages. This article proposes to carry out an evaluation of the compressive strength and microstructural alterations of ternary mixtures using NS and MK at the ages of 1, 3, and 7 days. At all early ages, it was verified that the 13MK2NS paste showed superior compressive strength to the ordinary Portland Cement (OPC) paste and that the peak of C-S-H occurred more quickly with greater heat flow. From the TG/DTG and FTIR tests, there was a greater consumption of calcium hydroxide (CH) by the ternary mixture 13MK2NS, mainly after 3 days of hydration. From Si^{29} NMR, it was also verified that the synergistic effects between NS and MK favors a greater incorporation of aluminium in the C-A-S-H structure at ages 1, 3, and 7 days. The results indicate that the synergistic effect between MK and NS occurs continuously throughout hydration from 1 day of hydration to, more expressively, 7 days.

KEYWORDS: *Nanosilica, metakaolin, synergistic effects, C-A-S-H*

I. INTRODUCTION

Supplementary cementitious materials (SCM) have been used by the cement industry as a strategy to reduce the clinker content of the types of cement produced [1-9]. Among the alternatives of supplementary cementitious materials (SCM) for the production of High-Performance Concrete (HPC), the use of metakaolin (MK) and nanosilica (NS) in isolation allows the formation of a more efficient composite. Metakaolin (MK) is a pozzolanic material originating from the calcination of kaolinite clays at temperatures ranging from 500 to 800 °C, while nanosilica (NS) is a nanoscale technology that has been introduced as an advanced pozzolan [10].

The incorporation of MK causes changes in the chemical composition of hydrate with the formation of C-A-S-H. When considering that the constitution of MK is high in aluminum, the incorporation of aluminum into the C-A-S-H structure can be considered as one of the reasons that affect the properties of the cementitious structure [11-14]. When analyzing the mechanical properties of mixtures with MK, it is observed that there is a decrease in resistance at ages of 3 and 7 days, with replacement levels between 10 and 20%. This can be attributed to the pozzolanic reaction in MK not being well developed at these ages and the filler effect not being able to repair the clinker reduction. Neto et al. [20] mentions that MK can also modify the hydration kinetics of the mixture, increasing the probability of undersulfation occurring.

Among the available nanomaterials, authors such as Roychand et al. [21] cite nanosilica as a material with high potential for improving the properties of cement composites. Garcia-Taengua et al [22] mentions that NS properly dosed in the cement mixture is capable of increasing the performance of the mixture through 3 mechanisms, filler effect, nucleation effect and pozzolanic effect, and these mechanisms can be observed through modifications in the cement matrix at early ages.

An increase in the performance of the cement matrix can be achieved with the joint use of MK and NS, both in terms of mechanical resistance and material durability [23-26]. Furthermore, changes in the microstructure are evident from the analysis of the C-S-H/C-A-S-H formed, highlighting the synergy of these two materials [19, 27-34]. These studies show that there is a better synergistic effect between MK and NS, reflecting increased compressive strength and microstructural changes, such as high CH intake and increased mean chain length (MCL) of C-S-H/C-A-S-H.

Jamsheer et al. [27] addresses the aspect that the use of NS in the cement mixture favors the formation of a more refined porous structure and, additionally, the introduction of MK into the mixture increases the probability of formation of C-A-S-H. Authors such as Sousa and Rêgo [34] evaluated the nanosilica/metakaolin ratio in the formation of C-A-S-H and through the parameter f. They observed that in the ternary mixture about 1/5 of the tetrahedral sites were occupied by aluminum. Jamsheer et al. [27] and Sousa and Rêgo [34] found that after 28 days, the average size of the C-A-S-H chain was higher in ternary mixtures, compared to reference and binary mixtures.

Although some studies present analyses of mixtures containing MK and NS, none of these studies have proposed to understand the age at which synergy has already been verified between these two components deeply. Considering that no researches are focusing on the hydration of mixtures containing MK and NS in the initial ages, this article proposes to complement the research esplanade on the theme of ternary cement mixtures, developing a study that evaluates hydration in the initial ages 1, 3 and 7 days of ternary mixtures of Portland cement containing MK and NS.

II. METHODOLOGY

2.1. Materials

The materials used in this article were: Type V Portland Cement (OPC), according to Brazilian Standard NBR 7215 (1996), HP Ultra Metacaulim (MK) produced by Metacaulim do Brasil, Colloidal Nanosilica (NS) with 30% solids content, produced by AkzoNobel; and Superplasticizing Additive (SP), Master-Glenium 51 produced by BASF.

To use the colloidal NS, drying was carried out in an oven for 48h to perform the loss of ignition (LOI) test. The chemical compositions of OPC, MK and NS are presented in Table 1, obtained by X-ray fluorescence spectroscopy (XRF). From the OPC and MK laser granulometry test, an average diameter of 14.05 µm and 15.85 µm, respectively, was observed. The specific surface area of OPC, MK and NS was 1.00 m²/g, 18.05 m²/g, 80m²/g, respectively.

Table 1. Chemical and physical composition of OPC, MK and NS cement

Properties		OPC	MK	NS
	SiO_2	20.85	58.1	94.84
	Al_2O_3	4.64	33.28	0.15

Chemical composition (%)	MgO	5.10	0.12	<0.01
	Fe_2O_3	3.08	2.21	<0.01
	Cao	58.33	0.11	<0.01
	In_2O	0.39	-	1.96
	K_2O	1.05	1.62	<0.01
	TiO_2	0.25	1.47	<0.01
	P_2O_5	0.16	0.11	<0.01
	MnO	<0.01	-	<0.01
	SO_3	4.07	0.11	-
	Other	<0.01	-	<0.01
	Loss of ignition	2.69	2.38	3.10
Granulometry	d10 (µm)	2.63	2.06	-
	d50 (µm)	12.51	12.17	-
	d90 (µm)	45.00	71.00	-
	Average diameter (µm)	14.05	15.85	-
Specific surface (m^2/g)		1.00	18.05	80*
Density (g/cm^3)		3.05	2.56*	-

*Data provided by manufacturer

X-ray diffraction patterns were also found for OPC (Fig. 1.a), NS (Fig. 1.b) and MK (Fig. 1.c). A Bruker D8 Discover difameter with voltage of 40kV and amperage of 40mA was used. The sweep speed was 15 rpm, from 3 to 100º 2θ. Compounds such as larnite (C2S), tricalcium silicate (C3S), anhydrous calcium ferroaluminate (C4AF), gypsum and tricalcium aluminate (C3A) were found in the cement diffractogram. No peaks were detected in NS test, highlighting the amorphous nature of the material. Additionally, the X-ray diffraction test was carried out in MK, as shown in Figure 1c, in which the compounds quartz, kaolinite, anatase and muscovite were identified. The identified kaolinite indicates that there is still a quantity of this compound that did not undergo crystalline change after burning, to form reactive metakaolinite, represented by the amorphous halo.

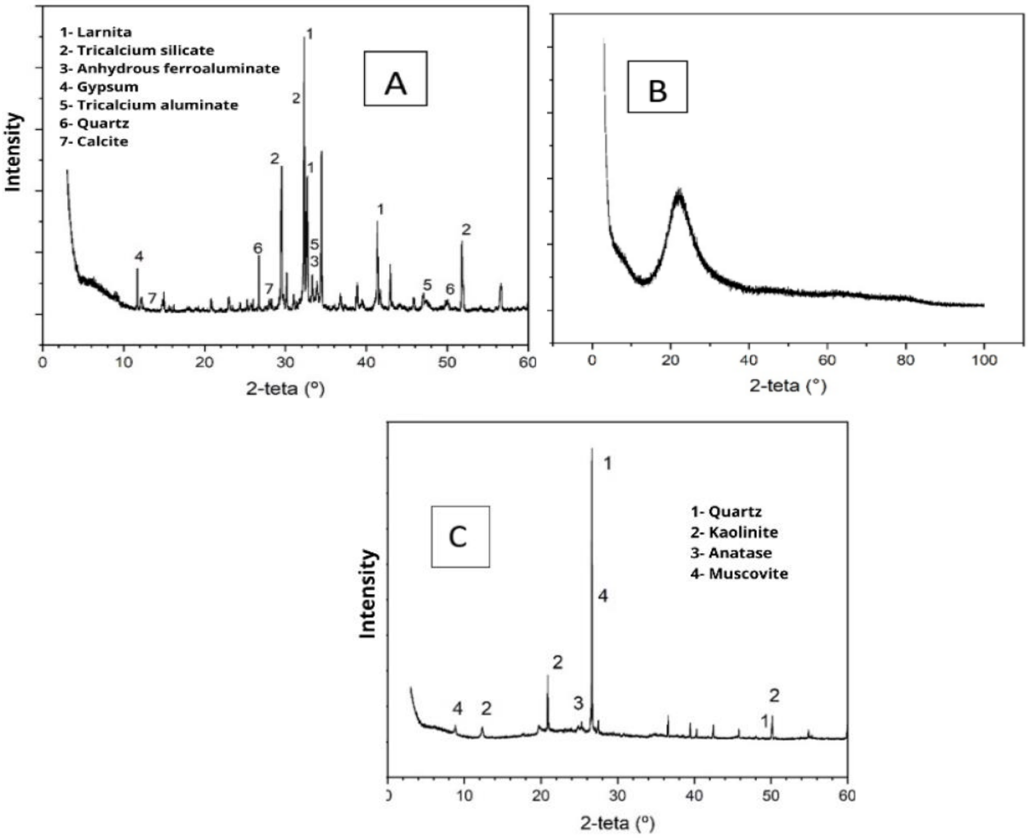

Figure. 1. Difratograms obtained from cement (a) OPC where: 1- Larnita (C_2S); 2- Tricalcium silicate (C_3S); 3 – Anhydrous calcium ferroaluminate (C_4AF); 4- Gypsum;5 - Tricalcium achloride (C_3A), 6- Quartz (SiO_2), 7-

Calcite ($CaCO_3$); (b) NS amorphous; (c) MK where: 1- Quartz (SiO_2); 2- Kaolinite ($Al_2Si_2O_5(OH)_5$); 3- Anatase (TiO_2); 4- Muscovite (KAl_2 $(Si_3Al)O_{10}$ $(OH. F)_2$.

2.2. Preparation and composition of pastes

To achieve this study objectives, the pastes needed to be analyzed at three different ages: 1, 3, and 7 days. The consistency of the pastes, measured by the mini-slump test [35], was fixed at 94±10mm, and the content of the superplasticizer was changed in each paste to achieve the determined consistency (table 2). The water content of colloidal NS and superplasticizer additive were subtracted from the total water content to maintain the same w/b ratio of 0.40 for all pastes.

The pastes were prepared in a planetary mortar mixer, with the following procedure: first, the water/NS/SP mixture was added to the mixer and then the previously homogenized OPC and MK mixture. Later, the materials were homogenized with the slow rotation of the mixer (140rpm) for 60 seconds and then with the rapid rotation (280rpm) for 90 seconds. The paste was used to shape cylindrical specimens, 50mm in diameter and 100mm in height. The specimens were placed in a humid chamber for 24 h, demolded and then cured by immersion in aqueous solution saturated with lime until the ages of testing. This procedure followed the Brazilian Standard NBR 7215/1996 with adaptations.

For each paste, 4 specimens were used for the compressive strength test. The quantitative and composition of the pastes produced are shown in Table 2. It is notable that, for the composition of the paste with NS, the water present in colloidal nanosilica solution (30% solids content) was considered, so that the water/cement ratio of 0.4 was maintained. With the materials used in the preparation of the pastes, the mixing procedure was performed to perform the isothermal calorimetry test, and after the rupture of the specimens, samples were collected for x-ray diffraction (XRD), thermogravimetric analysis (TG), Fourier transform infrared spectroscopy (FTIR) and nuclear magnetic resonance (NMR 29Si). The hydration of the samples was interrupted by immersion in isopropanol for 24 h, followed by drying at 40ºC for 6h. After hydration paralyzed, the samples were involved in plastic film and stored in closed containers with silica gel and soda lime, to limit the interactions with moisture and CO_2 until the age of the tests. Table 2 shows that to maintain the same spreading, the paste that required the most superplasticizer additive was 13MK2NS, followed by the binary paste of MK (15MK) and the reference (OPC). The behavior presented is coherent, considering the high specific surface of the NS and low particle size of the SCM. The high SP content of the ternary paste can be justified by the combined effect of these materials.

Table 2. Composition of the pastes produced in the study

Pastes	Abbreviation	OPC (g)	MK (g)	NS content (%)	NS (g)	Colloidal NS solution (g)	SP (%)	Mini-slump diameter (mm)	Water (g)
100%OPC	OPC	2400	-	-	-	-	0.21	93.2	957.0
85%OPC + 15%%MK	15MK	2040	360	-	-	-	1.05	102.7	950.59
85%OPC+13%MK +2%NS	13MK2NS	2040	312	2	48	160	1.62	94.6	825.05

2.3. Test carried out

All tests were performed at 1, 3, and 7 days of hydration. The tests of compressive strength of the specimens were performed in a universal test machine, according to Brazilian Standard NBR 7215/1996.

Isothermal calorimetry was performed with an eight-channel TAM air (TA Instruments) Thermometric calorimeter, with a computerized data acquisition system, average reading frequency every 30 seconds, and controlled temperature of 23ºC for 72 h.

TGA was performed in samples of ground pastes using a Thermal Analyzer TA Instruments SDT Q60 q0. The initial mass of the samples of 10±1mg was placed in a platinum crucible, the test was performed between 50 and 800°C with a heating rate of 10°C/min, with an N2 flow of 100mL/min. From the

TG/DTG curves, the CH content was calculated from equation 1, and the CH index, which is the parameter that relates the CH content of the reference paste with the other pastes at the specified ages.

CH content = 4,11 * volatilized water content Equation 1 [36]

The FTIR was performed in the range of 4000-400cm^{-1} with samples of ground pastes. They were mixed with KBr (ratio 1:100). Data were recorded with a Bruker Vertex 70 spectrometer.

The ^{29}Si NMR was performed with an Ascend 600 Avance III HD Model Bruker Console, equipped with a 4 mm CP/MAS H/X probe and an applied DT magnetic field of 14.1 T (600 MHz). The test was performed at the turning frequency of 10KHz, with a pulse duration of 4.25µs and pulse interval of 10s, using a minimum of 1024 points to have each spectrum. Tetramethylsilane (TMS) was used as an internal reference. The spectra obtained were deconvoluted in their elementary components with the Software TopSpin 4.1.3 Bruker, using Gaussian/Lorentzian profiles. After the deconvolution of the spectra, using the relative areas of each Qn component, it is possible to calculate two parameters that characterize the C-S-H, mean chain length (MCL) and parameter f, use for measure the fraction of spaces in the chain filled by aluminum tetrahedrons. These parameters are calculated using equations 2 and 3 [37]:

$$MCL = \frac{2}{\left(\frac{Q1}{Q1 + Q2(0Al) + \frac{3}{2}Q2(1Al) + Q3(0Al) + Q3(1Al)}\right)} \qquad \text{Equation 2}$$

$$f = \frac{\frac{1}{2}Q2(1Al)}{\frac{3}{2}Q1 + Q2(0Al) + \frac{3}{2}Q2(1Al) + Q3\ (0Al) + Q3\ (1Al)} \qquad \text{Equation 3}$$

III. RESULTS AND ANALYSIS OF RESULTS

3.1. Compressive strength

Table 3 presents the results of the compressive strength of the pastes produced in the study, as well as the Performance Index (PI) of the pastes produced, which is paste compressive strength compared to the strength of the OPC paste at the specified age. Table 3 also presents the homogeneous groups obtained with the Duncan Test. The ANOVA test was also performed, considering the pastes compositions as the independent variable and the compressive strength as the dependent variable, the results are shown in Table 4. It was verified that the pastes composition was significant in compressive strength at 1, 3 and 7 days, since the p-value found was lower than the confidence level 0,05.

Table 3 - Results of compressive strength of the pastes produced and Duncan test homogeneous at 1, 3 and 7 days

Age	Paste	Mean compressive strength (MPa)	Performance index (PI) (%)	Group 1	Group 2	Group 3
1 day	OPC	21,2	100	X		
	15MK	17,1	80,5	X		
	13MK2NS	32,8	154,6		X	
3 days	OPC	40,0	100	X		
	15MK	31,2	78,0	X		
	13MK2NS	44,1	110,1		X	
7 days	OPC	43,2	100	X		

	15MK	44,8	103,7	X	X	
	13MK2NS	55,0	127,4			X

Table 4 – ANOVA test parameters at 1, 3 and 7 days of hydration

Age	Dependent variable	Independent variable	*p*-value	Significance
1 day	Paste composition	Paste composition	0,000005	Yes
3 days	Paste composition	Paste composition	0,000925	Yes
7 days	Paste composition	Paste composition	0,017839	Yes

With 1 day of hydration, the 13MK2NS paste presented the highest compressive strength value with 32.8 MPa and PI of 154.6% (Group 2). This behavior of the paste that used NS can be justified by the three effects that this nanomaterial promotes: filler effect, nucleation effect, and pozzolanic effect, as cited by Wang et al. [38] and García-Taengua et al. [32], evidencing the importance of NS in this parameter. At this same age of evaluation, the 15MK paste presented lower IP with 80.5% (Group 1). This may be related to the pozzolanic reaction and, consequently, additional C-A-S-H production, which has not yet developed at this age, and by the lower clinker content in the paste.

At 3 days of hydration, the 15MK paste continued to present a lower PI of the OPC paste, with a performance index of 78.0% (Group1), according to the results obtained by Rêgo et al. [28] and Shafiq et al. [29]. The highest PI was evidenced in the 13MK2NS paste with 110.1% (Group 2).

The decrease in the performance index at 3 days of sample 13MK2NS compared to 1 day may be associated with a decrease in NS activity, given the high probability that a significant amount of NS has already reacted, so that the pozzolanic reaction attributed to MK has not yet started, as has the C-S-H layer on the clinker surface, which blocks hydration. [39-42].

The low-strength behavior of the 15MK paste at 3 days begins to change at 7 days, where the results of compressive strength are matched with the OPC paste, considering that at this age the pozzolanic reaction of the MK begins to intensify [43]. From 7 days, the 15MK paste exceeds the strength result of the OPC paste, presenting an ID of 103.72% (Group 2). At 7 days, the 13MK2NS paste presented an increase in ID 127.4% (Group 3), indicating the intensification of the pozzolanic reaction of MK in this period.

3.2. Isothermal calorimetry

The calorimetric curves evidencing the heat flow up to 72 h of the three pastes produced in this study are shown in Figure 2. It is possible to observe changes in the profile of the 15MK and 13MK2NS curves along all stages of hydration when compared to the OPC, as seen in the parameters in Table 5.

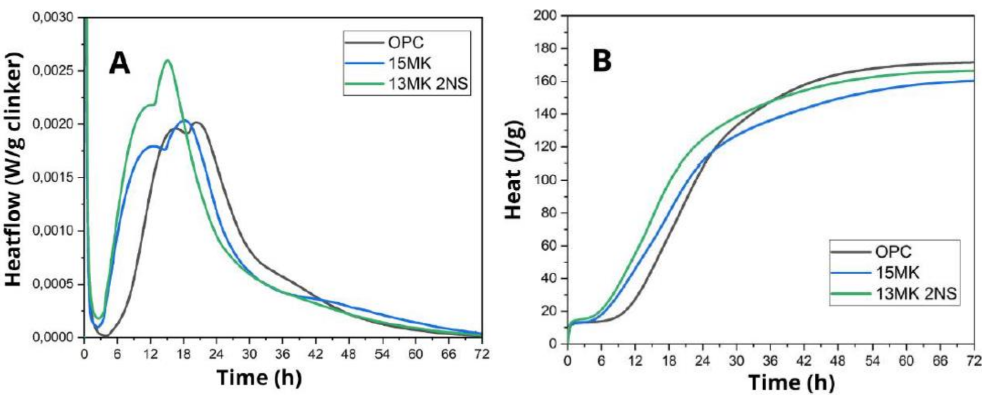

Figure. 2 (a) Normalized heat flow of pastes up to 72 h of hydration and (b) Accumulated heat of the pastes produced with 72h of hydration.

Table 5 - Isothermal calorimetry analysis parameters

Sample	**OPC**	**15MK**	**13MK 2NS**
Test time (h)	72	72	72
Time of end of dissolution (h)	0.2759	0.2128	0.2118
Induction end time (h)	7.09	3.15	3.38
C-S-H peak heat flow (mW/g)	1.962	1.795	2.181
C-S-H peak time (h)	16.7	12.62	11.96

When analyzing the heat flow of the C-S-H peak, it was verified that the paste 13MK2NS presented the highest value, being the values of 2.181 mW/g, results that corroborate those pointed out by Antoni et al. [39], Scrivener et al. [44], Andrade et al. [19] and Zunino and Scrivener [45]. It is also noteworthy that all pastes with SCM had a formation of the peak of C-S-H occurring significantly earlier compared to the OPC mixture (16.70h).

When analyzing the 13MK2NS paste in Figure 2, it is possible to notice the formation of the admixture peak closer to the Peak of C-S-H, which shows that in this paste the phenomenon of undersulfation occurred [20-46]. This undersulfation behavior of the 13MK2NS paste can be explained by the study by Zunino and Scrivener [45], in which the authors verified that the use of SCM increases the specific surface of the matrix, and this helps the occurrence of subsulfation, taking into account that the nucleation effect increases the precipitation of C-S-H, which causes sulfate ions to be absorbed on the C-S-H surface

When analyzing the total accumulated heat of the pastes with 24h, the 13MK2NS paste presented the highest accumulated heat value in the initial hydration period up to 24h, evidencing the contribution of NS to the increase of accumulated heat, justified by the characteristics of the high reactivity of this material. With 3 days of hydration, the highest total accumulated heat of the pastes followed the decreasing order: OPC, 13MK2NS, and 15MK, as seen in Figure 2. The lowest accumulated total heat values were identified in the pastes containing MK, which is explained by the decrease in hydration of C3S, due to the substitution of 15% of clinker in pastes with MK and by the pozzolanic reaction of MK has not yet occurred in greater intensity at 3 days of hydration.

3.3. Thermogravimetry (TG/DTG)

The TG/DTG curves of the pastes tested at the ages of 1, 3, and 7 days are shown in Figure 3, respectively. The evaluation and comparison of the calculated CH contents and the CH index to the OPC pastes are shown in Table 6.

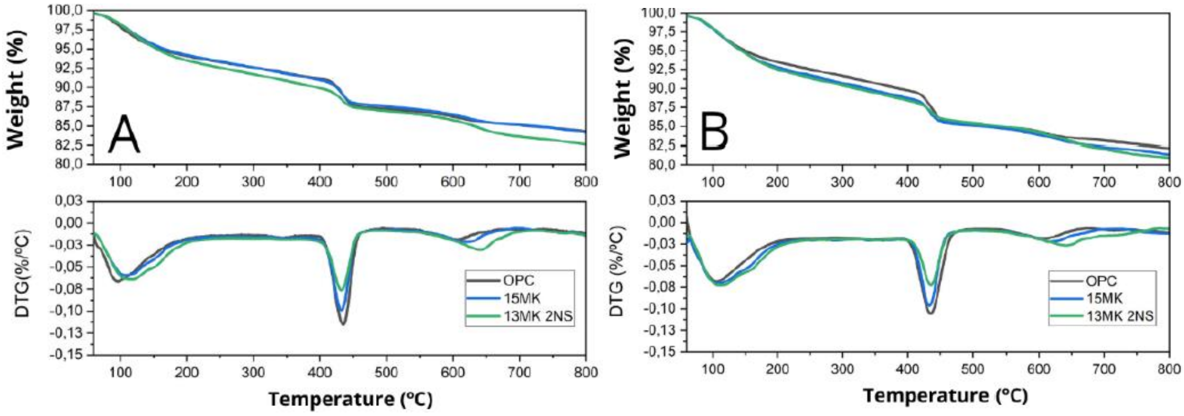

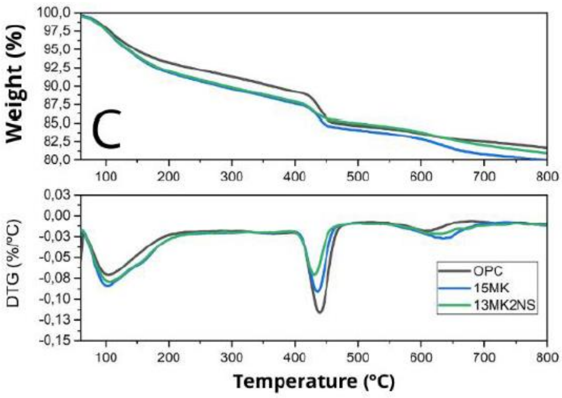

Figure. 3 TG and DTG curves of pastes with (a) 1 day hydration, (b) 3 days and (c) 7 days

Table 6 - Parameters obtained from mass loss and DTG curves at ages 1, 3 and 7 days

PASTES	1 day			3 days			7 days		
	CH (%)	T.CH (%)	I.CH	CH (%)	T.CH (%)	I.CH	CH (%)	T.CH (%)	I.CH
OPC	3.61	14.83	100	4.22	17.36	100	4.29	17.64	100
15MK	3.57	14.68	98.96	3.16	12.98	74.80	2.94	12.08	68.50
13MK2NS	3.26	13.39	90.29	2.69	11.07	63.79	2.53	10.40	58.93

With 1 day of hydration, the lowest I.CH was evidenced in the 13MK2NS paste, with 90,29%. Singh et al. [46] attributes this behavior of high CH consumption of pastes with NS, mainly to the nucleation effect provided by this nanomaterial and also to the high specific surface area, as pointed out by Zhao et al. [47]. The 15MK paste, presented I.CH 98,96, attributed to the acceleration of clinker hydration by increasing nucleation points, favoring hydration without running the pozzolanic reaction of MK.

At 3 days of hydration, the behavior of pastes with SCM presented lower I.CH compared with the OPC paste is observed. The lowest I.CH were evidenced in the pastes 13MK2NS and 15MK, 63,79% and 74,80%, respectively. At this age, it is already possible to observe the onset of pozzolanic reactions of MK that led to an increase in CH consumption in the 15MK paste at 3 days concerning 15MK paste with 1 day.

At 7 days, it is possible to verify that the ternary paste 13MK2NS presents a high consumption of CH with the lowest I.CH, 58,93% among all pastes produced at all ages, which reinforces the synergy between the components already mentioned above. The behavior of the ternary paste indicates that while the chemical reaction of NS tended to stabilize at 3 days, the effects of MK on the paste occurred, thus promoting the formation of an intersection point. These results are in agreement with the studies of Sousa [34], which presented I.CH of these ternary pastes MK/NS at 7 days of 61.61% and 55.17%, for pastes with different MK/NS ratios.After 1, 3 and 7 days, the levels of hydrated phases were evaluated based on the mass loss in the range of 50 to 450°C, which is related to the dehydroxylation of the main phases formed during the Portland cement hydration process [48-50]. The hydrated phase content was used to calculate a Hydrated Phase Index (HP index) for the pastes, which directly compares them with the OPC paste. Table 7 compiles the results.

3.4. Infrared spectroscopy (FTIR)

Figure 4 shows the FTIR spectra of the OPC, 15MK, and 13MK2NS samples with 1, 3, and 7 days of hydration. For the evaluation of the hydrates formed, two regions were analyzed, the one referring to CH at peak 3643 cm^{-1} and C-A-S-H at peak 971 cm^{-1}. Taking into consideration the semiquantitative character of the technique, the transmittance values indicate the contents of each compound of the pastes, so the lower the transmittance value, the greater the amount of the compound in the matrix.

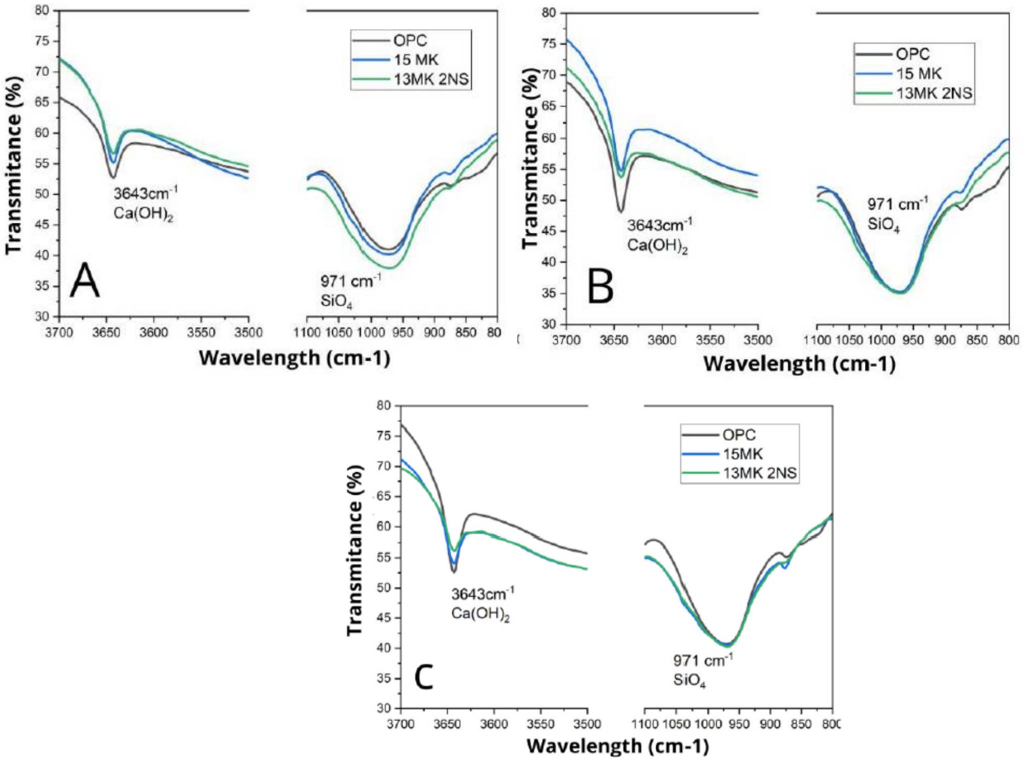

Figure. 4 Infrared spectra in the CH and C-S-H regions with (a) 1 day hydration, (b) 3 days hydration and (c) 7 days hydration

The semi-quantitative method of FTIR applied in this study was that proposed by Andrade et al. [19]. These authors verified that at 28 days, there was a decrease in the intensity of the peak of CH, which reflects on CH consumption, of ternary pastes when compared to the other pastes produced with other SCM. This behavior described at 28 days was verified in this study at the ages of 1, 3, and 7 days, as seen in the spectra of Figure 4.

When evaluating the spectrum region referring to CH at the ages of 1, 3, and 7 days, it is verified that the transmittance values are lower for the OPC paste, justified by the absence of a compound that reacts with CH in the cement matrix, which reflects the absence of CH consumption, followed by the 15MK and 13MK2NS pastes.

When analyzing the spectrum region referring to C-S-H at ages 1, 3, and 7 days, it was verified that the lowest transmittance values were detected in the 13MK2NS paste, suggesting the greater formation of C-S-H/C-A-S-H, a result that is in line with those of compressive strength presented in table 3.

Studies that have been published on the theme of ternary pastes with MK and NS evaluate cementitious matrices only at the age of 28 days. Jamsheer et al. [27] observed that the use of NS and MK promoted an elongation in the Si-O bond, which is directly related to the incorporation of aluminum in the C-S-H chain. This elongation in the Si-O bond indicating that the inclusion of aluminum in the C-S-H chain has been happening since the first day of hydration, when compared to the other pastes, can be seen in 13MK2NS pastes at 1, 3, and 7 days.

3.4. Nuclear magnetic resonance imaging (^{29}Si NMR)

The ^{29}Si NMR results containing their respective deconvoluted spectra and the curves resulting from the deconvolutions of the peaks used for analysis are shown in Figures 5, at the ages of 1 day, 3 days, and 7 days hydration. Table 7 gathers the results of 29Si NMR for pastes produced at the ages of 1, 3, and 7 days.

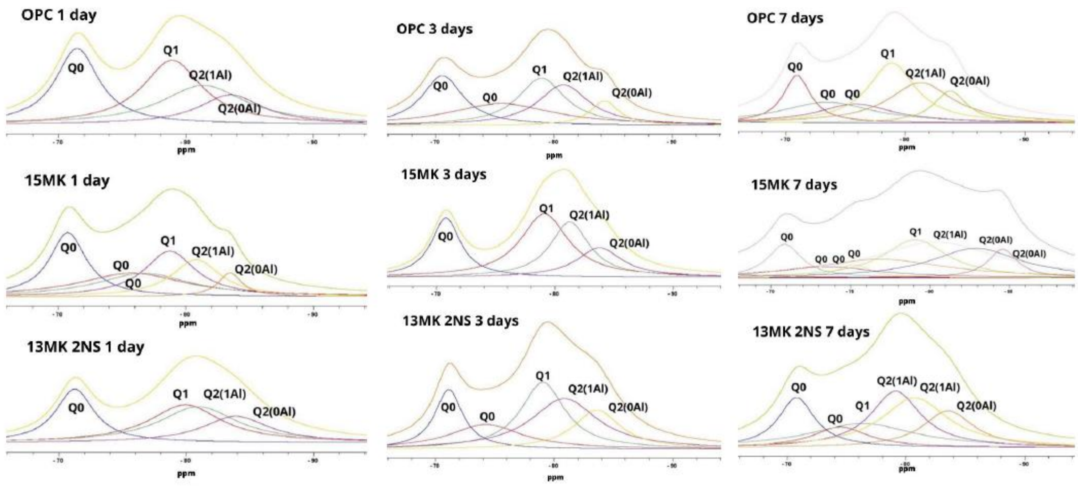

Figure. 5 Results of ^{29}Si NMR for the pastes produced with 1 day, 3 days and 7 days

Table 7- MCL and parameter f for OPC, 15MK and 13MK2NS pastes at ages 1, 3 and 7 days.

Age	Pastes	MCL Richardson [37]	Parameter f
1 day	OPC	5.57	0.131
	15MK	4.76	0.132
	13MK2NS	6.36	0.140
3 days	OPC	5.36	0.144
	15MK	4.98	0.117
	13MK2NS	6.65	0.149
7 days	OPC	5.45	0.140
	15MK	10.33	0.162
	13MK2NS	10.78	0.207

When evaluating the initial hydration period at the age of 1 day, the highest values of MCL with 6.36 in the 13MK2NS paste were verified. This behavior can be justified by the high reactivity of NS and rapid initial reaction that favors the entry of silicon into the C-S-H structure, already evidenced by the studies by Pérez et al. [49] and by the results of mechanical strength (Table 3). The MCL results of the 13MK2NS paste indicate that in this period there is already a synergistic interaction between NS and MK, considering that even with lower clinker content (85%) the paste 13MK2NS can stand out in the MCL value when compared to the other pastes.

It is noteworthy that with 1 day of hydration, the 15MK paste did not reach an MCL value similar to the OPC paste, which evidences a slower reactive behavior of this paste at this age, also taking into account the low consumption of CH obtained from the TG/DTG tests (Table 6), and the low compressive strength at this same age (Table 3).

At 3 days of hydration, the 15MK paste showed an increase in the MCL value to the age of 1 day, however, there was still a lower value than the OPC paste. The 13MK2NS paste presented the highest MCL value, reflecting the increase in the relative area of Q2, to the other pastes with 3 days of hydration and, mainly, in the Q2(1Al) fraction, resulting from the insertion of aluminium from the C-S-H chain.

Additionally, it is possible to verify a trend of progressive increase of MCL in 15MK and 13MK2NS pastes, since the pozzolanic reaction of MK starts at 3 days and intensifies from days of hydration. At

7 days of hydration, the pastes 13MK2NS and 15MK presented the highest values of MCL, with 10.78 and 10.33, respectively. When analyzing the results presented in Table 7, it is proven that the combination of MK and NS promotes changes in the chemical structure of C-A-S-H since 1 day of hydration, presenting the highest values of MCL with 1, 3, and 7 days, when compared with the other pastes.

Table 7 presents the f parameter values, corresponding to the amount of aluminum inserted from the structure of C-S-H/C-A-S-H, of the pastes at the ages of 1, 3, and 7 days. Considering that parameter f measures the fraction of spaces in the chain filled by aluminum tetrahedrons, it is observed that the ternary paste 13MK2NS generated a higher f value, with 0.140, 0.149, and 0.207 to 1, 3, and 7 days, respectively, which demonstrates the effect of NS, in facilitating the inclusion of aluminum in the C-A-S-H chain. Moreover, with the results of parameter f, it can be assumed that around 20% of the tetrahedron spaces are needed for aluminum tetrahedron in the C-A-S-H composition, as seen by Sousa and Rêgo [34] at 28 days.

IV. CONCLUSIONS

By analyzing the results in this article, it is possible to reach the following conclusions.

At the initial ages of 1, 3, and 7 days, the use of NS was a fundamental factor for compressive strength gain. The ternary mixture 13MK2NS showed higher compressive strength among the pastes, which evidences the synergy between these materials, whereas even with the replacement of 15% of clinker it was possible to obtain mechanical results superior to the OPC paste.

The paste 13MK2NS showed heat release and a more accelerated reaction, compared to the other, evidenced by the formation of the peak of C-S-H/C-A-S-H more rapidly. Considering that the 13MK2NS paste had undersulfation, it is possible to infer that the results of mechanical strength of the sample at the ages of 1, 3, and 7 days could have been greater if there had been a balance of sulfate in the cementitious matrix;

The quantitative (TG/DTG) and semi-quantitative (FTIR) results of calcium hydroxide (CH) intake showed that the ternary paste (13MK2NS) showed the most expressive behavior in the consumption of CH from the pozzolanic reaction, among the pastes produced, mainly from the 3 days of hydration.

Although the isolated use of MK did not contribute to the increase of the MCL of the C-S-H/C-A-S-H chain with 1 and 3 days of hydration, the combined use with NS favored the progressive increase of MCL, indicating the importance of NS for aluminum incorporation for the formation of C-A-S-H since 1 day hydration.

The chemical changes resulting from the synergy of these SCM, such as high consumption of calcium hydroxide (CH), incorporation of aluminum in the C-S-H/C-A-S-H chain and increase in MCL, directly influenced the mechanical properties of the paste produced, which resulted in compounds with more efficient performance when compared to the others. Thus, the results indicate that the synergistic effect of MK and NS occurs continuously throughout the hydration period, starting from 1 day, due to the contribution of NS, and intensifying from 3 days onwards, due to the contribution of MK.

ACKNOWLEDGEMENTS

The authors wish to thank the financial support provided by the National Council for Scientific and Technological Development (CNPq/Brazil), the National Council for the Improvement of Higher Education (CAPES/Brazil), the Federal District Research Support Foundation (FAPDF/Brazil), CYTED Ibero-American program of science and technology for development, and the University of Brasilia (UnB/Brazil).

REFERENCES

[1] Scrivener K.L., Avet, F., MAraghechi, H., Zunino, F., Ston, J., Hanpongpun, W., Favier, A. (2019). "Impacting factors and properties of calcined clay cements (LC3)" Green materials, 7.3-14.

[2] Benkeser, D.; Hernandez, K.; Lolli, F.; Kurtis, K. (2022) "Influence of Calcined Clay Morphology on Flow in Blended Cementitious Systems." Cem. Concr. Res., 160, 106927.

[3] Bonavetti, V.L.; Castellano, C.C.; Irassar, E.F. (2022) "Designing General Use Cement with Calcined Illite and Limestone Filler." Appl. Clay Sci. 230, 106700.

[4] Mencía, R.V.; De La, V.; Frias, M.; Ramírez, S.M.; Carrasco, L.F.; Giménez, R.G. (2022) "Concrete/Glass Construction and Demolition Waste (CDW)." Materials, 15, 4661.

[5] Boris, R.; Wilinska, I.; Pacewska, B.; Antonoviˇc, V. (2022) "Investigations of the Influence of Nano-Admixtures on Early Hydration and Selected Properties of Calcium Aluminate Cement Paste." Materials, 15, 4958.

[6] Becerra-Duitama, J.A.; Rojas-Avellaneda, D. (2022) "Pozzolans: A Review. Eng. Appl. Sci. Res."

[7] Sevinç, A.H. (2022) "Investigating the Properties of GGBFS Hazelnut Ash–Based Cement-Free Mortars Produced at Ambient Temperature under Different Curing Conditions." J. Mater. Civ. Eng., 34, 4022268.

[8] Durgun, M.Y.; Sevinç, A.H. (2022) "Determination of the Effectiveness of Various Mineral Additives against Sodium and Magnesium Sulfate Attack in Concrete by Taguchi Method." J. Build. Eng., 57, 104849.

[9] Eduardo, C.; Balestra, T.; Rocha, L.; Jubanski, E.; Nakano, A.Y.; Helena, M.; Schneider, R.; Angel, M.; Gil, R. (2023) "Contribution to Low-Carbon Cement Studies: Effects of Silica Fume, Fly Ash, Sugarcane Bagasse Ash and Acai Stone Ash Incorporation in Quaternary Blended Limestone-Calcined Clay Cement Concretes." Environ. Dev, 45, 100792.

[10] Majstorović, F., Sebera, V., Mrak, M., Dolenec, S., Wolf, M., and Marrot, L. (2021) "Impact of metakaolin on mechanical performance of flax textile-reinforced cement-based composites." Cement and Concrete Composites, 126.

[11] Siddique, R.; Klaus, J. (2009) "Influence of metakaolin on the properties of mortar and concrete: A review." Applied Clay Science, v. 43, n. 3–4, p. 392–400.

[12] Mo, Z., Wang, R., & Gao, X. (2020) "Hydration and mechanical properties of UHPC matrix containing limestone and different levels of metakaolin." Construction and Building Materials, 256.

[13] Kocak, Y. (2020) "Effects of metakaolin on the hydration development of Portland–composite cement." Journal of Building Engineering, v. 31, p. 101419.

[14] Bahmani, H., and Mostofinejad, D. (2022) "Microstructure of ultra-high-performance concrete (UHPC) – A review study." Journal of Building Engineering, 50 (January).

[15] Mermerdaˉs, K., Gesoǧlu, M., Güneyisi, E., Özturan, T. (2012) "Strength development of concretes incorporated with metakaolin and different types of calcined kaolins." Build. Build. Mater. 37, 766–774.

[16] Shah, S.P., Bhattacharyya, S.K., Mishra,G., ET al. (2015) "Studies on early-stage hydration of tricalcium silicate incorporating silica nanoparticles: Part II." Constr. Build. Mater. 102, 943–949.

[17] Borosnyói, A. (2016) "Long term durability performance and mechanical properties of high-performance concretes with combined use of supplementary cementing materials." Build. Build. Mater. 112, 307–324.

[18] Dadsetan, S., Bai, J. (2017) "Mechanical and microstructural properties of self-compacting concrete blended with metakaolin, ground granulated blast-furnace slag and fly ash." Build. Mater. 146, 658–667.

[19] Andrade, D. Da Silva; Silva Rêgo, J. H. DA; Cesar Morais, P.; Frías Rojas, M. (2018) "Chemical and mechanical characterization of ternary cement pastes containing metakaolin and nanosilica." Construction and Building Materials, v. 159, p. 18–26.

[20] Neto, J.S.A; Santos, T.A.; Pinto, S.A.; Dias, C.M.R.; Ribeiro, D.V. (2021) Effects of the combined use of carbon nanotubes (CNT) and metakaolin on the properties of cementitious matrices. Construction and Building Materials 271 (121903).

[21] Roychand, R.; Silva, S.DE; Setunge, S. (2018) "Nanosilica modified high-volume fly ash and slag cement composite: Environmentally friendly alternative to OPC." Journal of Materials in Civil Engineering, v. 30, n. 4.

[22] García-Taengua, E; Sonebi, M; Hossain, K.M.A; Lachemi, M; Khatib, J. (2015) "Effects of the Addition of Nanosilica on the Rheology, Hydration and Development of the Compressive Strength of Cement Mortars." Composites Part B, Vol. 81, pp. 120–129.

[23] Gaitero, J.J., Campillo, I., Guerrero, A. (2008) "Reduction of the calcium leaching rate of cement paste by addition of silica nanoparticles." One hundred. Res. 38, 1112–1118.

[24] Tobón, J.I., Payá, J.J., Borrachero, M.V., Restrepo, O.J. (2012) "Mineralogical evolution of Portland cement blended with silica nanoparticles and its effect on mechanical strength." Build. Build. Mater. 36, 736–742.

[25] Duan, P.; Shui, Z.; Chen, W.; Shen, C. (2013) "Effects of metakaolin, silica fume and slag on pore structure, interfacial transition zone and compressive strength of concrete." Construction and Building Materials, v. 44, p. 1–6.

[26] Li, L. G., Zhu, J., Huang, Z. H., Kwan, A. K. H., & LI, L. J. (2017) "Combined effects of micro-silica and nano-silica on durability of mortar." Construction and Building Materials, 157, 337–347.

[27] Jamsheer, A.F.; Kupwade-Patil, K.; Büyüköztürk, O.; Bumajdad, A. (2018) " Analysis of engineered cement paste using silica nanoparticles and metakaolin using 29Si NMR, water adsorption and synchrotron X-ray Diffraction." Construction and Building Materials, v. 180, p. 698–709.

[28] Rêgo, J. H. DA S.; Rojas, M.F.; Terrades, A.M.; Fernández-Carrasco, L.; Morales, E. R.; Rojas, M.I.S.DE. (2019) "Effect of partial substitution of highly reactive mineral additions by Nanosilica in cement pastes." Journal of Materials in Civil Engineering, v. 31, n. 1, p. 1–11.

[29] Shafiq, N.; Kumar, R.; Zahid, M.; Tufail, R. F. (2019) "Effects of modified metakaolin using nano-silica on the mechanical properties and durability of concrete." Materials, v. 12, n. 14.

[30] Andrade, D.; Silva Rêgo, J. H. DA; Morais, P.C.; Mendonça LOPES, A. N. DE; Rojas, M. F. (2019) "Investigation of C-S-H in ternary cement pastes containing nanosilica and highly-reactive supplementary cementitious materials (SCMs): Microstructure and strength." Construction and Building Materials, v. 198, p. 445–455.

[31] Sousa, M. I. C.; Silva Rêgo, J. H. DA; Martirena-Hernandez, J. F.; alujas-díaz, A.; Amador-Hernandez, M. (2020) "Mechanical Strength Analysis of Ternary Cement Pastes Containing Nanosilica and Metakaolin." Brasília, DF 910-900, Brazil: Springer Netherlands, v. 22.

[32] Garcia, R.; Henao, N.; La Rubia, M.A. DE; Moragues, A.; Fernandez, J. (2020) "Early contributing nanostructured cementitious matrix designs: Benefits in durable features at early ages." Construction and Building Materials, v. 241.

[33] Mena, J.; González, M.; Remesar, J. C.; Lopez, M. (2020) "Developing a very high-strength low-CO2 cementitious matrix based on a multi-binder approach for structural lightweight aggregate concrete." Construction and Building Materials, v. 234.

[34] Sousa, M. I. C., and Rêgo, J. H. DA S. (2021) "Effect of nanosilica/metakaolin ratio on the calcium alumina silicate hydrate (C-A-S-H) formed in ternary cement pastes." Journal of Building Engineering, January 38.

[35] Kantro, D. (1980) "Influence of Water-Reducing Admixtures on Properties of Cement Paste." Cement, Concrete and Aggregates, v. 2, n. 2, p. 95-102.

[36] Scrivener, K., Snellings, R. and, & Lothenbach, B. (2016) A Practical Guide to Microstructural Analysis of Cementitious Materials. Civil Aeromedical Research Institute (U.S.).

[37] Richardson, I. G. (2014) "Model structures for C-(A)-S-H(I)." Acta Crystallographica Section B Structural Science, Crystal Engineering and Materials, v. 70, n. 6, p. 903–923.

[38] Wang, Y; XU, Z; Wang, J; Zhou, Z; Du, P; Cheng, X. (2019) "Synergistic effect of nano-silica and silica fume on hydration properties of cement-based materials." Journal of Thermal Analysis and Calorimetry.

[39] Antoni, M., Rossen, J., Martirena, F., Scrivener, K.L. (2012) "Cement substitution by a combination of metakaolin and limestone." Cement and Concrete Research, 42, p.1579-1589.

[40] Meng, T., Hong, Y., Wei, H., Xu, Q. (2019) "Effect of nano-SiO 2 with different particle size on the hydration kinetics of cement." Thermochim. Acta 675, 127–133..

[41] Raheem, A. A., Abdulwahab, R., & Kareem, M. A. (2021) "Incorporation of metakaolin and nanosilica in blended cement mortar and concrete- A review." Journal of Cleaner Production, 290.

[42] Althoey, F., Zaid, O., Martínez-garcía, R., Alsharari, F. (2023) "Impact of Nano-silica on the hydration , strength , durability , and microstructural properties of concrete : a state-of-the-art review" Case Studies in Construction Materials Impact of Nano-silica on the hydration , strength , durability , and microstructural properties of concrete : a state-of-the-art review. Case Stud. Constr. Mater. 18, e01997

[43] Flores, Y. C. et al. (2017) Performance of Portland cement pastes containing nano-silica and different types of silica. Construction and Building Materials, v. 146, p. 524–530.

[44] Scrivener, K.L. (2014) "Options for the Future of Cement". Indian Concr. J., 88, 11–21.

[45] Zunino, F. Scrivener, K. (2019) "The influence of filler effect on the sulfate requirement of blended cements." Cement concre. Res. 162, 105918.

[46] Ruviaro, A. S., Silvestro, L., Scolaro, T. P., DE Matos, P. R., and Pelisser, F. (2021) "Use of calcined water treatment plant sludge for sustainable cementitious composites production." In Journal of Cleaner Production (Vol. 327).

[46] Singh, L. P.; Bhattacharyya, S.K.; Shah, S.P.; Sharma, U. (2015) "Studies on Hydration of tricalcium Silicate Incorporating Silica Nano-particles." Springer International Publishing Switzerland. Nanotechnology in Construction.

[47] Zhao, L.; Guo, X.; Liu, Y.; Ge, C.; Guo, L.; Shu, X.; Liu, J. (2017) "Synergistic effects of silica nanoparticles/polycarboxylate superplasticizer modified graphene oxide on mechanical behavior and hydration process of cement composites." The Royal Society of Chemistry, 7, 16688–16702.

[48] Pérez, G. et al. (2014) "Structural characterization of C-S-H gel through an improved deconvolution analysis of NMR spectra." Journal of Materials Science, v. 49, n. 1, p. 142–152.

Authors

Master's degree in the Postgraduate Program in Structures and Civil Construction (PECC) at the University of Brasília (UnB). Graduated in civil engineering at the Federal University of Pará (UFPA). As an undergraduate, he was a member of the Civil Construction Materials Research Group (GPMAC), where he worked on the reuse of waste for the production of concrete and also with self-compacting and permeable concrete. He is interested in the following areas: nanomaterials, supplementary cementitious materials, eco-efficient cements and concrete technology. He works as a concrete technologist, developing, optimizing and reviewing conventional and special concrete traits.

He is a professor at the Federal Institute of Education, Science and Technology of Goiás - Campus Formosa, where he works mainly in the area of Civil Construction Materials and Construction Technology. He has a Technical Course in Buildings (CEFET-Go, 2007), a degree in Civil Engineering (PUC-GOIÁS, 2010), Specialization in Construction and Project Management (UNIP, 2013), a Master's degree in Structures and Civil Construction (UnB, 2016) and PhD in Structures and Civil Construction (UnB, 2023). He participates in research in the area of new materials and supplementary materials for Portland cement.

Graduated in Civil Engineering from the Federal University of Goiás (1996), Master's degree in Civil Engineering from the Federal University of Goiás (2001), PhD in Structures and Civil Construction from the University of Brasilia (UnB), Post-Doctorate PRODOC at the Federal University of Goiás (2007), Post-Doctorate at the Polytechnic University of Catalonia (2017) and Post-Doctorate at the Eduardo Torroja Institute of Construction Sciences (Madrid/Spain) (2023). He is currently Associate Professor III at the Department of Civil and Environmental Engineering at UnB and a CNPq Scholarship Modality: Research Productivity PQ-2. He has experience in the area of Civil Engineering, with an emphasis on Construction Materials, working mainly on the following topics: Supplementary Cementitious Materials, Pozzolans, Portland Cement, Agroindustrial Waste, Construction and Demolition Waste, Circular Economy, Concrete Microstructure, Construction Pathology, Microstructural analysis techniques, Nanosilica, Nanotechnology of cementitious materials

Graduated in Civil Engineering, he completed his doctorate in the Postgraduate Program in Civil Engineering at the Federal University of Santa Catarina in 2010. He was an adjunct professor at the University of Extremo Sul Catarinense, working in the Civil Engineering and Architecture and Urbanism courses, and in the Program of Postgraduate Studies in Materials Science and Engineering, from 2002 to 2015. He is currently an adjunct professor at UFSC - Federal University of Santa Catarina, working on the Civil Engineering course and the Postgraduate Program in Civil Engineering. CNPq research productivity scholarship. He has experience in the area of Civil Construction, with an emphasis on cementitious materials, working mainly on the following topics: nanostructure of cement, industrial waste applied to concrete and development of eco-efficient concrete. He participates in the Laboratory of Nanotechnology Applications in Civil Construction (Nanotec-Lab) and is leader of the Eco-efficient Concrete Research and Development Group. He supervised numerous works, including scientific initiation, course completion, specialization, master's and doctorate. He works as a reviewer for national and international journals, and as Associate Editor of the IBRACON Structures and Materials Journal.

PhD in chemistry from the Autonomous University of Madrid. Scientific Researcher at Institute of Eduardo Torroja for Construction Sciences (IETcc-CSIC). Work experience mainly in the valorization of industrial by-products and wastes as pozzolanic additions for the manufacture of cements and concretes, from the scientific, technical and environmental viewpoint (reaction kinetics, evolution of hydrated phases, modeling of pozzolanic reaction (kinetic-diffusive and thermodynamic models), microstructure, new eco-cementing matrices, durability, expansive compounds, allergenic components (soluble chromium,.). monographs (9) and, books+ book chapters (>15).

Full Professor at the E.T.S.I. of Roads, Canals and Ports of the U.P.M since 1987. PHd in Chemical Sciences, Complutense University of Madrid, 1995. Graduate in Chemical Sciences, Literary University of Valencia, 1980. Basically focused on two lines of Research: Construction materials and Environmental pollution caused by road traffic